Research Article **Open Access**

Biosynthesis of silver-gold nanocomposites using *Aspergillus fumigatus* ND2 OR636497 and *Aspergillus flavus* ND1 OR636491 and evaluation of their biological activities

Dalia M. Abdelrahman[1], Nashwa H. Abdullah[1*], Ehab B. Eldomany[2], Ahmed H. Moustafa[3], Mohamed E. Osman[1]

[1]Botany and Microbiology Department, Faculty of Science, Helwan University, Cairo, Egypt; [2]Biotechnology and Life Sciences Department, Faculty of Postgraduate Studies for Advanced Sciences, Beni-Suef University, Egypt; [3]The Holding company for biologicals and sera (VACSERA), Giza, Egypt.

***Corresponding author:** Nashwa H. Abdullah, PhD, Botany and Microbiology Department, Faculty of Science, Helwan University, Cairo, Egypt

Submission Date: April 18th, 2024; **Acceptance Date:** June 22nd, 2024; **Publication Date:** June 27th, 2024

Please cite this article as: Abdelrahman D. M., Abdullah N. H., Eldomany E. B., Moustafa A. H., Osman M. E. Biosynthesis of silver-gold nanocomposites using Aspergillus fumigatus ND2 OR636497 and Aspergillus flavus ND1 OR636491 and evaluation of their biological activities. *Bioactive Compounds in Health and Disease* 2024; 7(6): 325-344.
DOI: https://www.doi.org/10.31989/bchd.v7i6

ABSTRACT:

Background: Recently, synthesis and use of innovative nanomaterials in food packaging industries has gained great interest not only in reducing the incidence of foodborne pathogens but also in preventing the changes of food ingredients that can be resulted from microbial growth and contamination.

Objective: Our study concerned with the design of silver-gold bimetallic nanoparticles to provide an innovative strategy for improving the antibacterial activity of gold nanoparticles and reduce the toxicity of silver nanoparticles yielding a promising bimetallic nanocomposite for food packaging and biomedical applications.

Methods: In the current study, metal-contaminated soil has been utilized in a trail to isolate new fungal isolates with good metal redox potential for metallic nanoparticles production. Size, shape, metal ratio, surface charge, nature of compounds involved in the formation and capping of the produced Ag-Au

nanocomposites were estimated. Antimicrobial and cytotoxic behavior of these nanocomposites has been tested.

Results: New *Aspergillus fumigatus* and *Aspergillus flavus* isolates with good potential for Ag-Au bimetallic nanocomposite production have been isolated. The produced nanocomposites showed sphere-like polyhedron shape, 10-25 nm size range, and exhibited the truncated tetrahedron pattern as the most common topographical pattern. Gold was the major metal in the nanocomposite synthesized by *Aspergillus fumigatus* ND2 OR636497 but *Aspergillus flavus* ND1 OR636491 nanocomposite showed a reversed case. Both nanocomposites recorded good surface charge value (-29.0 ± 2.3 & -27.3 ± 0.4) that can support a reasonable stability for the prepared nano solution. They exerted a good inhibitory effect against all tested Gram-negative and Gram-positive bacteria and showed significant antifungal behavior. In a trial to evaluate the safe applicability of the biosynthesized Ag-Au nanocomposites and to estimate their anticancer potential, their cytotoxic effect against a normal and cancer cell line has been evaluated. Results revealed their lower toxicity against the mice bone marrow cells and their elevated toxicity against MCF7 cell line with significant IC_{50} values.

Conclusion: This study provides efficient methods for green synthesis of Ag-Au nanocomposites utilizing new fungal isolates. Results revealed the safe and promising applicability of the biosynthesized Ag-Au nanocomposites in food packing as antimicrobial agent in addition to its promising anticancer activities.

Keywords: *Aspergillus fumigatus*, *Aspergillus flavus*, Ag-Au nanocomposite, antimicrobial, cytotoxicity, green synthesis.

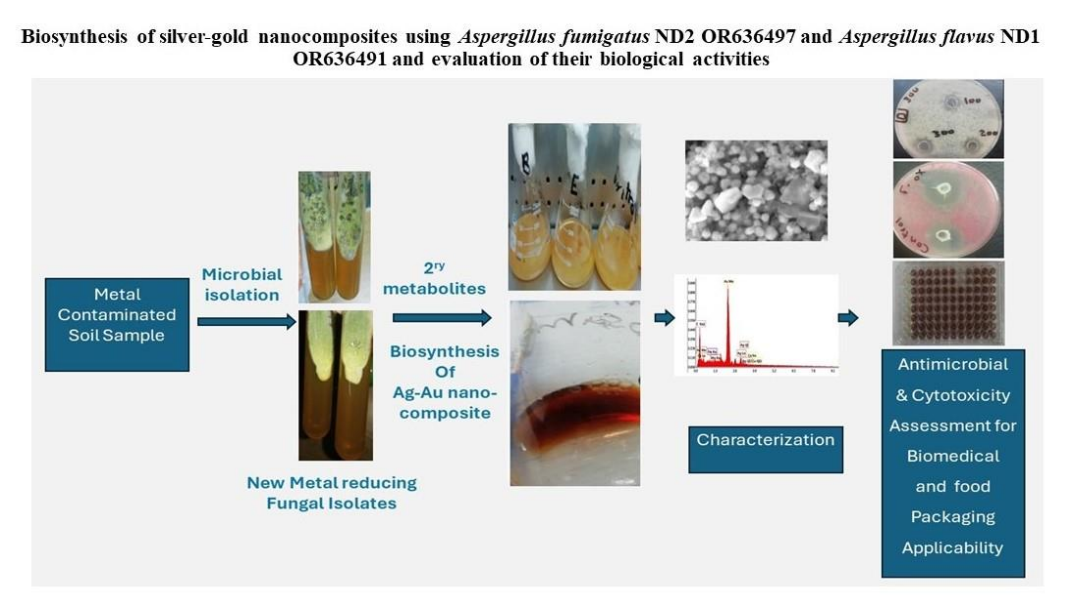

INTRODUCTION:

Nanomaterials (NPs) have received great attention due to their exceptional chemical, physical, and biological properties. Among these nanomaterials, metallic nanoparticles have garnered significant attention because of their advanced characteristics which make them appropriate for a wide range of applications [1- 2]. Generally, the properties of nanomaterials are determined by their size, shape, surface morphology, and composition [2]. According to their composition, metallic nanomaterials are usually synthesized as monometallic or bimetallic forms. Monometallic NPs contain only one type of metal and show distinct physical and chemical properties. Bimetallic NPs are obtained by combining two different types of metal in the structure of NPs yielding a novel variety of morphologies, structures, and features [3]. Recently, bimetallic nanocomposite materials have attracted great interest as they offer not only a combination of features that are correlated to the existence of their individual metals but also can add innovative features due to such dual metal association [4]. Combining two metals expands the range of the obtained forms, structure, and organization patterns [5]. Additionally, bimetallic nanoparticles interestingly exhibit more unique properties in comparison to their corresponding monometallic NPs due to the synergistic effect between the properties of two different metal parts [3]. Hence, recently researchers have focused on the synthesis of bimetallic nanoparticles in a trial to enhance the characteristics of the produced mono-metal NPs [6]. Tuning of bimetallic nanoparticles properties and optimization of their performance can be accomplished by the proper selection of metal combination and optimizing their ratio in the produced nanoparticles [3].

Nanoparticles of noble metals represent very important sector of nanomaterials owing to their unique features that support their potential applications in different fields such as medicine, water treatment, food packaging, chemical sensing, bioimaging, catalysis, nonlinear optical devices, drug delivery, and others [5]. Among these noble metals, silver and gold nanoparticles play a significant role in biological applications due to their attractive physiochemical features [7-8].

The use of nanomaterials that exhibit good antimicrobial activities in food packaging systems represents an innovative emerging technique. It provides a smart solution to extend the shelf life of food and prevent the change in its functional ingredients [9] which ensures their effective bioavailability [10]. Also, it can play a role in maintaining the desired quality of food and prevents the incidence of food borne diseases [9].

In food industry, silver nanoparticles have been used in new food packages and containers in a trial to exploit their anti-microbial potential [9]. On the other hand, gold nanoparticles have been reported to exhibit a significant role in reducing the microbial load in foodstuffs, thus they also have been recommended to be implemented in food packaging systems especially due to their inert and nontoxic nature [11].

Silver nanoparticles are interesting bioactive agents. They show strong toxicity against a wide range of microorganisms [7] and are effectively used in the production of antimicrobial textiles and antibacterial catheters [12]. Also, the cytotoxic potential of Ag nanoparticles is well documented [13]. However, recent studies have revealed that the wide usage of Ag monometallic nanoparticles can derive serious drawbacks on human health and the environment due to the accumulation of the cytotoxic silver ions released during the Ag NPs interactions [14-15]. That may impose limitations in its application especially with the appearance of resistant bacterial strains because of its continuous usage [16]. Although gold nanoparticles are considered as less toxic and safer nanoparticles, their applications are somewhat more limited due to their high-cost production and their lower antibacterial

activities. Hence the design of silver-gold bimetallic nanoparticles can provide an innovative strategy to improve the antibacterial activity of Au NPs and reduce the toxicity of Ag NPs [8]. However, to date, only a few studies have estimated the synthesis of the Ag-Au bimetallic nanocomposites and assessed their effectiveness in biological applications.

The anticipated dual action of the combined metals in bimetallic nanoparticles is very intriguing since it can change and improve their applicability. Indeed, the Ag-Au bimetallic nanoparticles have been detected to exhibit an improved potential in biological applications in comparison to their corresponding single metal nanoparticles. The improved bioactivity of bimetallic nanoparticles can be attributed to their increased surface area and additional degree of freedom which can boost their adsorption and interaction power [6]. Additionally, they can show diverse mechanisms of action [3], unique mixing patterns [6], and new geometrical architecture [5-6], which improve their functionality [6].

The investigated antibacterial activities of Ag-Au NPs can be, in part, owe to the synergic effect obtained between silver and gold atoms [5]. Indeed, in comparison to the monometallic Au NPs, bimetallic Au NPs showed improved antibacterial capabilities [17]. The existence of gold atoms on the Ag-Au nanocomposite can likely regulate the release of silver ions from the nanocomposite. Moreover, the addition of gold to silver nanoparticles can improve their inhibitory effect against bacteria that develop a resistant to Ag NPs due to their previous exposure to lower Ag. The continuous use of Ag nanoparticles has led to the development of resistance mechanisms in the treated bacteria such as their production of adsorbent protein that aggregates Ag NPs and that resulted in a clinical issue [16].

Generally, the physicochemical properties of bimetallic nanomaterials are determined by the used preparation techniques, which also regulate their size and shape [5]. Concurrent reduction of two metal ions with suitable stabilizing techniques is the common method for the synthesis of bimetallic nanocomposites [3].

Although synthesis of nanomaterials can be carried out using physical, chemical, or biological methods, biological synthesis of nanoparticles has gained great attention because physical and chemical methods either require harsh conditions, such as the use of high pressure and high temperature, using complex procedures, or utilize toxic chemicals that lead to negative environmental impacts [13]. Thus, attention has been shifted to the alternative “green” routes for the synthesis of nanoparticles. Such biological “green” synthesis methods provide an eco-friendly and cost-effective method using gentle safe and simple techniques [18]. Such biological synthesis processes usually utilize natural bioactive compounds derived from plants or microorganisms [19].

Because of their activities in the bioremediation of metals in nature, microorganisms have been efficiently used for metallic nanoparticles synthesis purposes. Moreover, in recent times, it has been proposed that the microbes' distinct characteristics could support them as efficient nanofactories. As a result, researchers are looking for microorganisms inhibiting various biological niches to find new species with special redox potential that may be used to reduce metal salts and create metallic nanoparticles [20]. Among these microorganisms, fungi provide efficient nanofactories. Compared to other microorganisms, fungi have a higher potential for secondary metabolites production which makes them a better tool for the synthesis of nanoparticles [13].

Hence this study aimed to isolate new fungal isolates inhibiting metal contaminated soils in a trail to provide new efficient nanofactories for green synthesis of Ag-Au nanocomposite. Additionally, the current study

aimed to estimate the antimicrobial and cytotoxic potential of the synthesized Ag-Au nanocomposites to evaluate their biomedical applicability and their applicability in food packaging systems.

METHODS:

Isolation and identification of fungal isolates: Fungal isolates utilized in this study were isolated from soil samples collected from the Iron and Steel Factory in Helwan- Egypt (29°46'47" N, 31°19'27" E). Isolation was carried out on Potato Dextrose agar medium "PDA" (Extract of 200 g potato slices, Dextrose 20.00, Agar 20 g/l, pH=5.6; [21]) and Czapek-Dox's agar medium (Sucrose 30.00, $NaNO_3$ 3.00, KH_2PO_4 1.00, $MgSO_4$ 0.50, KCl 0.50, $FeSO_4$ 0.01, Agar 20 g/l, pH=7.0; [22]) using serial dilution plate method [23-24]. The purified fungal isolates were identified molecularly by sequencing their ITS region using the ITS1 and ITS4 primers. DNA extraction and PCR reaction were conducted at Macrogen Company - Seoul - South Korea. The amplified sequences were analyzed by the Basic Local Alignment Search Tool (BLAST) provided by the National Center of Biotechnology Information (NCBI) website. Phylogenetic relationships were estimated using MegAlign (DNA Star) software version 5.05 and (NCBI) website.

Biosynthesis of Ag-Au nanocomposite: The efficiency of the investigated isolates for biosynthesis of Ag-Au nanocomposite has been estimated. Six fungal plugs (0.8 cm diameter) have been inoculated in 250 ml conical flasks containing 50 ml of culture medium described by Mahfouz *et al.*, 2016 [25] with slight modifications (Glucose 10.00, Yeast extract 5.00, KNO_3 2.00) and incubated at 28±2 °C for 14 days at 140 rpm. The obtained fungal biomass was harvested by filtration through Whatman filter paper no. 1. The collected biomass was washed with sterilized double distilled water, then 10 gm were re-inoculated in 50 ml sterile double distilled water contained in 250 ml conical flasks and incubated at 28±2 °C for 24 h at 140 rpm. Filtrate of this stage was separated from the biomass by filtration through Whatman filter paper no. 1 and used for nanocomposite synthesis. One ml of that filtrate was inoculated to 9 ml of an Au/Ag solution mixture (Tetrachloroauric (III) acid trihydrate ($HAuCl_4$) solution (60 mM): silver nitrate solution (1.5 mM) with 1:25 v/v ratio) and incubated at 28±2 °C for 48 h at 140 rpm. Nanocomposite formation was initially detected by observing the change in color of samples in comparison to salt-free control.

Characterization of the biosynthesized Ag-Au nanocomposite: The formation of Ag-Au NPs was initially detected by observing the visible color change from colorless to reddish brown and also by detecting its surface plasmon resonance (SPR) via the measurement of its UV-Visible spectrum at 200-800 nm range and comparing it to a control "sample free of salt" using JASCO V630 spectrophotometer. Further characterization was performed by employing Transmission Electron Microscopy TEM (JEM 2100 HRT, Japan, acceleration voltage of 200 KV) to visualize the shape and size of the synthesized nanocomposite. Additionally, Fourier Transform Infrared Spectroscopy FTIR (Perkin–Elmer, USA) was used to determine the types and nature of existing bonds and functional groups to verify the nature of compounds involved in the formation and capping of nanocomposite. FTIR Spectra were detected using scanning spectrum in the range 450–4,000 cm^{-1} at a resolution of 4 cm^{-1}. The type and percentage of elements in the prepared nanocomposite were monitored using EDX along with Scanning Electron Microscopy (JEOL, JSM-6360LA, Japan; coupled with an Energy Dispersive X-ray spectrometer). The surface charge of biosynthesized Ag-Au nanocomposite has been

measured by estimating its Zeta potential using nano-zeta sizer (Malvern ZS-Nano, Scattering angle of 90).

Effectiveness of the produced Ag-Au nanocomposite as antimicrobial agent:

Antibacterial activity*:* The antibacterial potential of the biosynthesized Ag-Au nanocomposite was evaluated against Gram-positive bacteria (*Streptococcus pneumoniae*, *Micrococcus luteus, Staphylococcus aureus* ATCC 25923, and *Staphylococcus aureus* ATCC 6538) and Gram-negative bacteria (*Escherichia coli* ATCC 7839 and *Salmonella typhi* ATCC 6539) using agar well diffusion method [26]. The tested bacteria were seeded on liquified warm nutrient agar medium and poured on sterilized Petri dishes (9 cm diameter). After solidification, wells were bunched on the agar medium by sterile cork borer (8 mm in diameter), and 100 µl from nanocomposite concentrations (100, 200, 300 ppm) was inoculated in these wells. The plates were incubated overnight at 4°C for diffusion of tested solutions then incubated at 37 °C for 24 h. Wells inoculated with sterile distilled water were tested as a negative control while discs loaded with 5 µg ciprofloxacin were used as a positive control. The inhibitory zone diameter was observed and measured (mm) to determine the antibacterial activity.

Antifungal activity: The antifungal potential of the biosynthesized nanocomposite was evaluated against five fungal plant pathogens (*Fusarium oxysporum*, *Fusarium solani*, *Fusarium semitectum*, *Alternaria solani* and *Rhizoctonia solani*). Ag-Au nanocomposite was tested in the concentration of (100, 200, and 300 ppm) using a well diffusion method. Warm Czapek-Dox's agar medium seeded with the tested fungi was poured on sterilized petri dishes. After solidification, wells were bunched on the agar medium using sterile cork borer and 100 µl of the tested nanocomposite concentration was inoculated on these wells. The plates were incubated overnight at 4°C for diffusion of tested solutions then incubated at 25 °C for 5 days. The inhibitory zone diameter was observed and measured (mm) to determine the antifungal activity.

Evaluation of cytotoxicity of synthesized Ag-Au nanocomposite: A normal cell line, mice bone marrow stromal cells (BM), and a cancer cell line, Human epithelial breast adenocarcinoma: MCF7 ATCC HTB 22, were used to test the cytotoxicity of the biosynthesized Ag-Au nanocomposite in the concentration range (300 – 9.4 ppm) using the MTT Cell Viability assay method [27]. Each concentration was tested in a triplicated manner and the average was calculated. Data were expressed as a percentage of relative viability compared to control cells. The following equation was utilized to calculate the percentage of relative viability:

(Absorbance of treated cells)/(Absorbance of control cells) ×100

By plotting the dose response curve, the average concentration required to kill 50% of the cell population, or the IC_{50} value, was estimated.

Statistical analysis: Tests were performed in replicated manner and mean values were expressed with their standard deviation values. Regarding the cytotoxicity test, data was displayed as mean value ± its SD, and by utilizing GraphPad Prism 9.4.1 (458) for MacOS, GraphPad Software, the dose-response curve was generated using non-linear regression analysis with five parametric logistic curve equations (San Diego, California USA, www.graphpad.com).

RESULTS:

Identification of fungal isolate: Sequencing of the amplified ITS regions of the investigated isolates, and their phylogenetic analysis revealed that; isolate number

1 shows 99.29: 99.46% similarity with different *Aspergillus fumigatus* strains and found with them in a common cluster, Figure 1-a. While isolate number 2 shows 99.28: 99.82% similarity with different *Aspergillus flavus* strains and is found with them in a common cluster, Figure 1-b. The morphological and microscopical features of these isolates were found to match this molecular identification data. Hence these isolates were identified as *Aspergillus fumigatus* isolate ND2 and *Aspergillus flavus* isolate ND1 and their sequences were submitted under the accession numbers of OR636497 and OR636491 respectively in the GenBank.

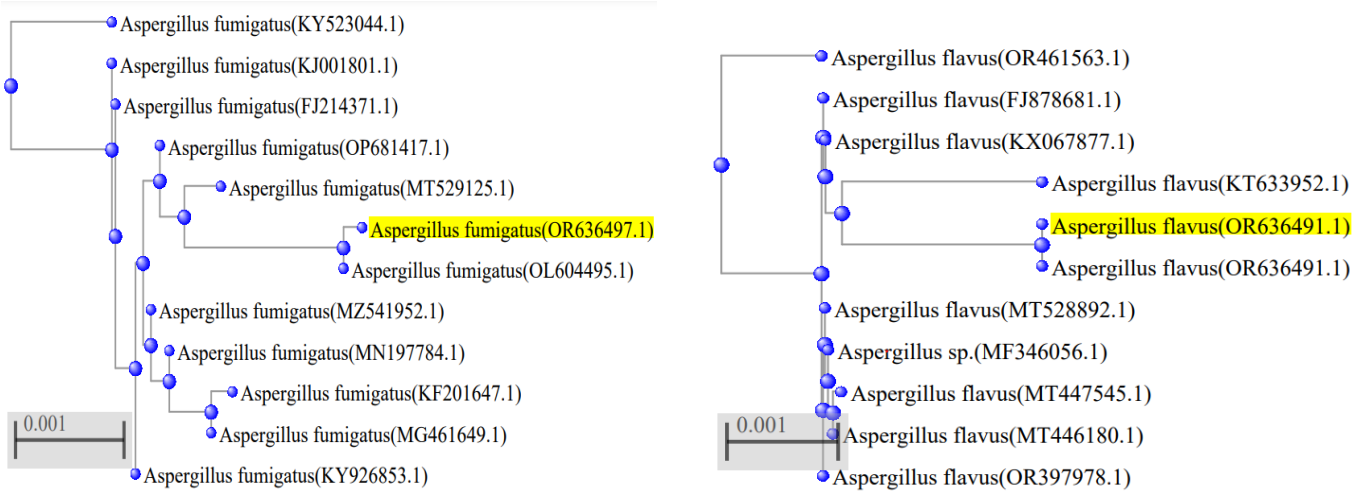

a): *Aspergillus fumigatus* ND2 OR636497 (b): *Aspergillus flavus* ND1 OR636491

Figure 1: Phylogenetic tree analysis of obtained sequences (NCBI); the analyzed sequences are highlighted.

Biosynthesis of Ag-Au nanocomposite: The formation of Ag-Au NPs was initially estimated by detecting the change in color and turning the color of the sample to reddish brown, Figure 2. Such color change represents a preliminary indication for the reduction of Ag and Au ions by the added filtrate and the production of the corresponding nanoparticles. Furthermore, the obtained UV–Vis spectrum has revealed the appearance of a characteristic peak for this Ag-Au nanocomposite at 440 nm, Figure 3.

Figure 2: Color change due to Ag-Au nanoparticles production.

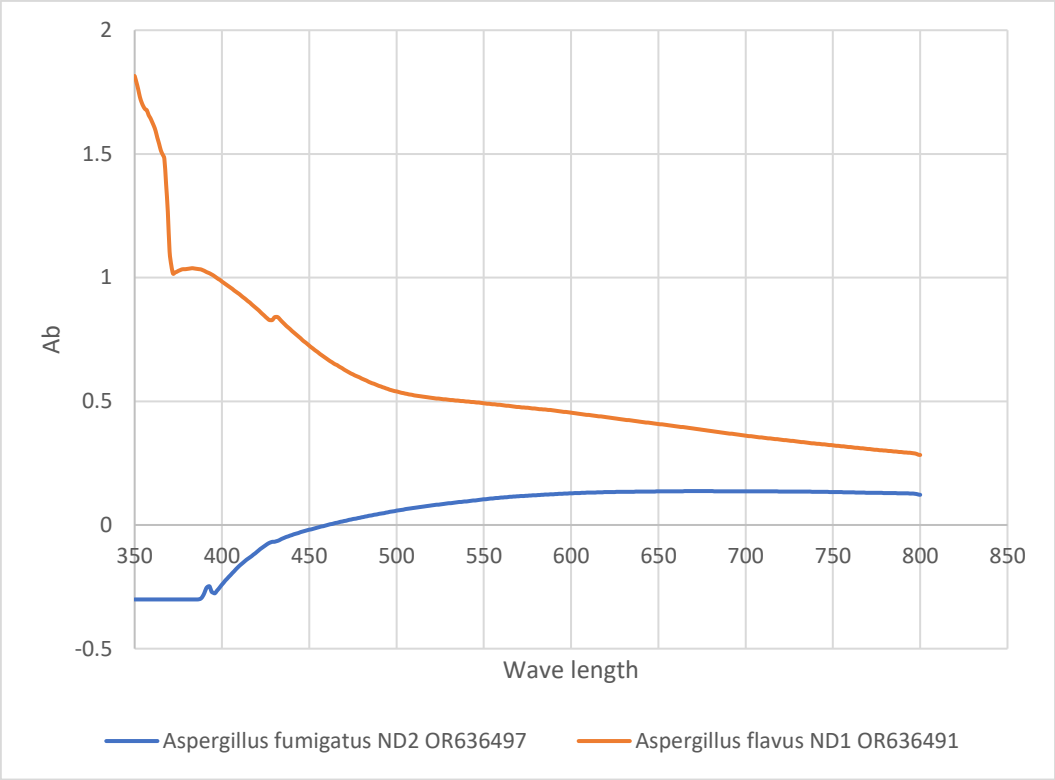

Figure 3: UV-Vis spectrum showing the formation of the Ag-Au nanocomposite beak.

Characterization of synthesized Ag-Au nanocomposite:

TEM: The obtained TEM graphs, Figure 4, showed the formation of sphere-like polyhedron nanoparticles and the majority of them with a size range 10-25 nm.

Zeta potential: Zeta potential analysis showed that the nanoparticles synthesized by *Aspergillus fumigatus* ND2 OR636497 have a surface charge of -29.0 ± 2.3 while those synthesized by *Aspergillus flavus* ND1 OR636491 their surface charge is -27.3 ± 0.4, Figure 5.

SEM & EDX: According to the obtained SEM micrographs, the truncated tetrahedron shape was recorded as the most common morphological shape among the biosynthesized nanoparticles, Figure 6.

The type and quantity of elements in the prepared nanocomposite have been monitored by employing energy-dispersive X-ray Spectroscopy (EDX) analysis. EDX spectra, Figure 7, revealed the presence of a strong absorbance peak at approximately 2.2 keV which is correlated to gold absorption and other beaks at nearly 3 keV which are characteristic to silver nanocrystal. These results confirm the successful preparation of Ag-Au nanocomposite. Another major beak has been reported for C in both samples. Silver and gold percentages in the biosynthesized nanocomposite samples were estimated. Gold is the major metal recorded in the nanocomposite synthesized by *Aspergillus fumigatus* ND2 OR636497 while silver is the minor one recording a percentage of 60.56% and 8.21% respectively. The relative content of these metals in nanocomposite synthesized by *Aspergillus flavus* ND1 OR636491, reported nearly a reversed ratio, where silver in this nanocomposite represents the major element (55.92%) and gold is the minor one (5.56%), Table 1.

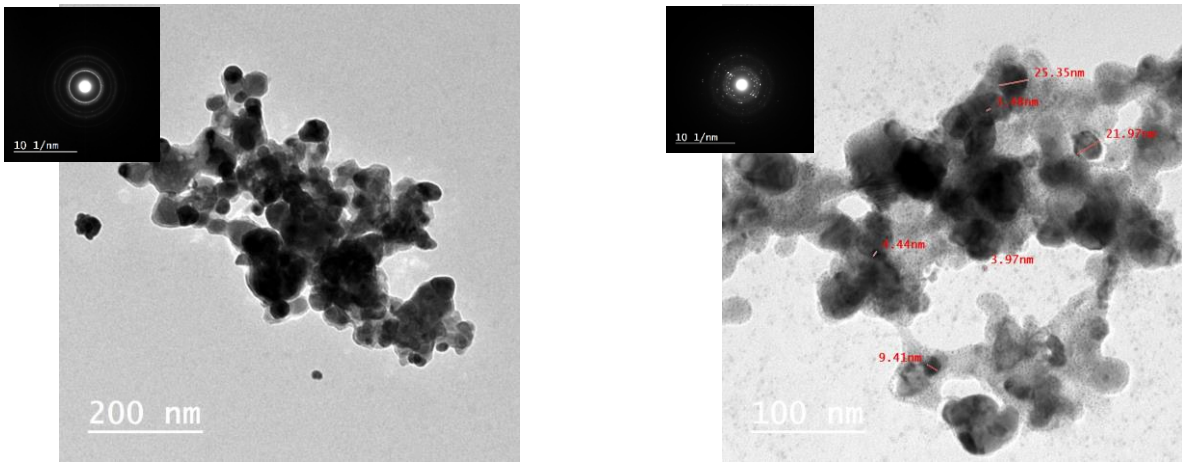

(a) **(b)**

Figure 4: TEM image of (a) *Aspergillus fumigatus* ND2 OR636497 and (b) *Aspergillus flavus* ND1 OR636491 mediated Ag-Au nanocomposite showing the electron diffraction pattern on the left top.

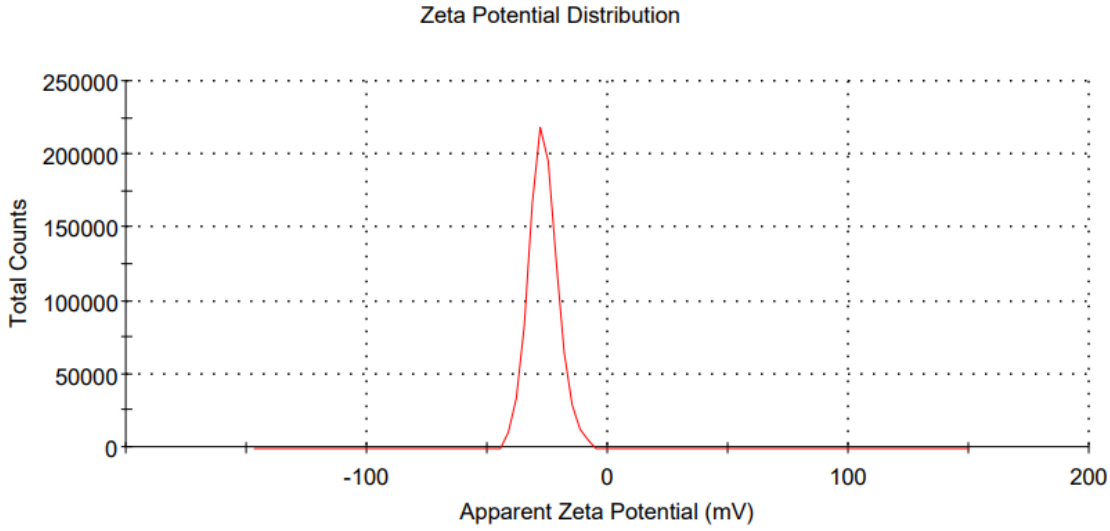

(a)

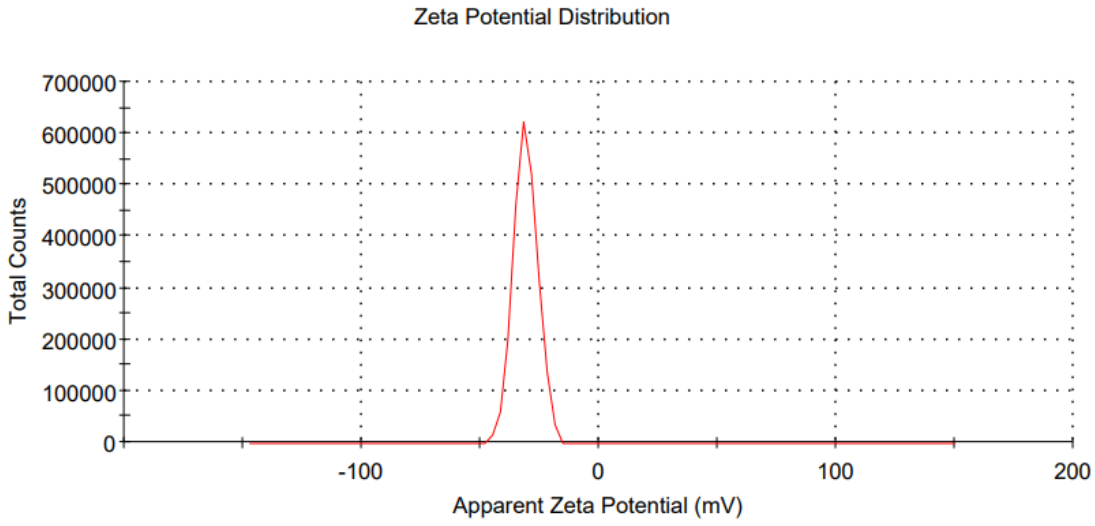

(b)

Figure 5: Estimation of surface charge of biosynthesized Ag-Au nanocomposite by measuring their Zeta potential **(a)** *Aspergillus fumigatus ND2 OR636497* **(b)** *Aspergillus flavus* ND1 OR636491.

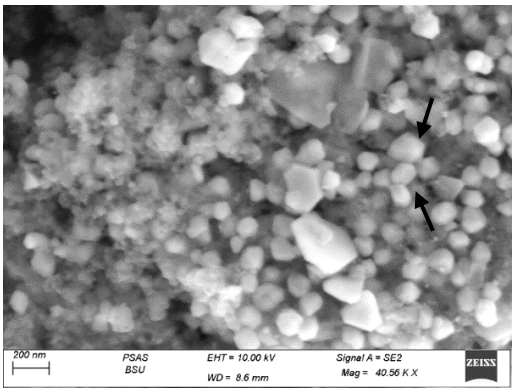

(a): *Aspergillus fumigatus* ND2 OR636497

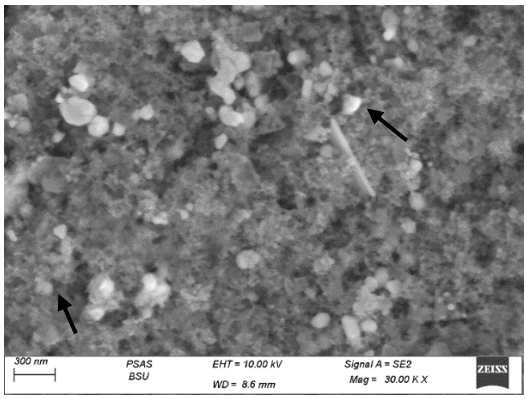

(b): *Aspergillus flavus* ND1 OR636491

Figure 6: SEM micrographs revealing the morphology of biosynthesized Ag-Au nanoparticles.

(a)

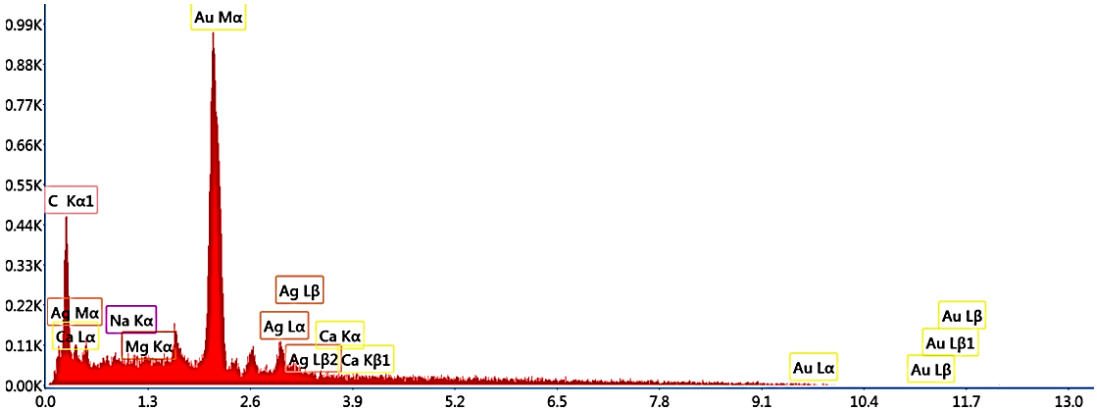

(b)

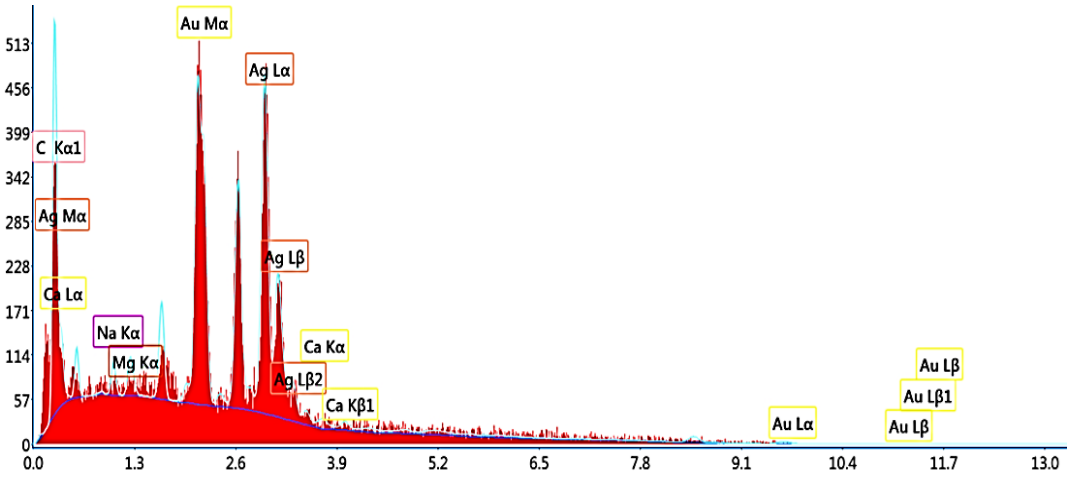

Figure 7: EDX Spectra showing silver and gold percentage in prepared samples. (a): *Aspergillus fumigatus* ND2 OR636497; (b): *Aspergillus flavus* ND1 OR636491

Table 1: EDX estimated elemental percentage in biosynthesized nanocomposite

Element (%)	C	Na	Mg	Ca	Au	Ag
***Aspergillus fumigatus* ND2 OR636497**	28.21	1.32	1.29	0.41	60.56	8.21
***Aspergillus flavus* ND1 OR636491**	31.85	3.76	2.34	0.49	5.56	55.92

FT-IR spectroscopy: FT-IR spectra of both nanocomposite samples showed common bands at 3755 3420, ~2920, 2860, 2375, ~1625, ~1391 and ~1046 cm^{-1}. A unique band has been reported at ~785 cm^{-1} for nanocomposite sample synthesized by *Aspergillus fumigatus* ND2 OR636497 and a unique band has been reported at ~1430 cm^{-1} for nanocomposite sample synthesized by *Aspergillus flavus* ND1 OR636491, Figure 8.

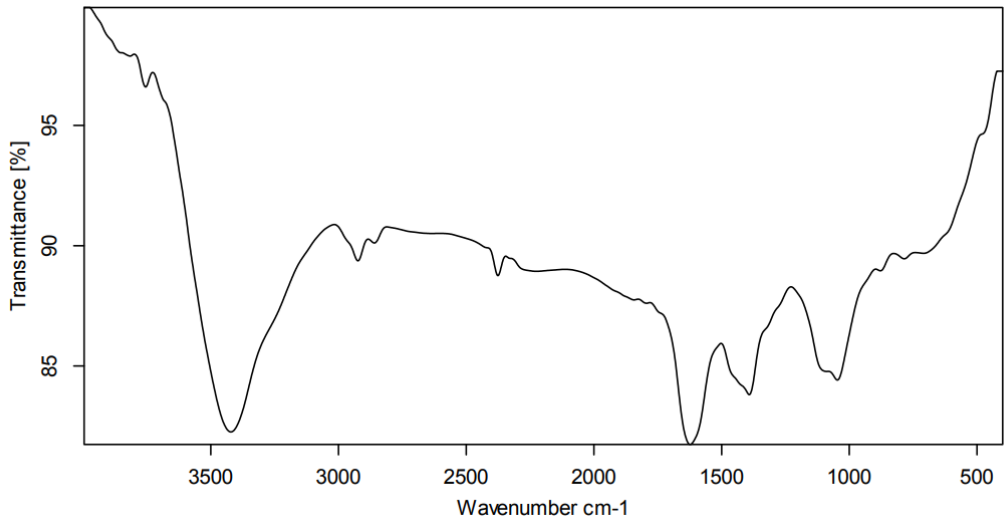

(a)

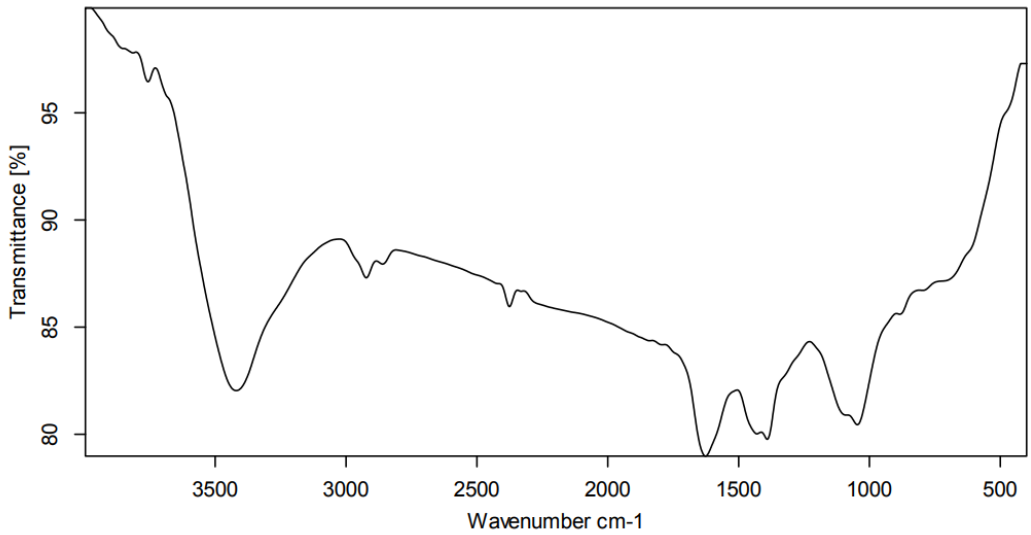

(b)

Figure 8: Fourier transforms infrared (FTIR) spectra of Ag-Au nanocomposite synthesized by; **(a)** *Aspergillus fumigatus ND2 OR636497* **(b)** *Aspergillus flavus* ND1 OR636491.

Effectiveness of the produced Ag-Au nanocomposite as an antimicrobial agent:

Antibacterial activity: Testing the antibacterial activity showed that the Ag-Au nanocomposites synthesized by both tested fungal isolates exert a good inhibitor effect against all tested bacteria. Ag-Au nanocomposite synthesized by *A. flavus* ND1 OR63649 in 300 ppm concentration has recorded the best inhibitory effect against most of the tested bacteria. However, Ag-Au nanocomposite synthesized by *A. fumigatus* ND2 OR63649 has recorded similar activity against *S. aureus* ATCC 6538 and exerted better activity against *S. aureus* ATCC 25923, Table 2.

Antifungal activity: Estimation of the antifungal activities of the biosynthesized Ag-Au nanocomposites revealed that they could exert antifungal activities against the tested fungal isolates. Ag-Au nanocomposite synthesized by both fungal isolates showed similar antifungal activities against the tested *Fusarium* species. However, Ag-Au nanocomposite synthesized by *A. fumigatus* ND2 OR63649 has recorded better antifungal activity against *Alternaria solani* while Ag-Au nanocomposite synthesized by *A. flavus* ND1 OR63649 has recorded the best inhibitory effect against *Rhizoctonia solani*, Table 3.

Table 2: Antibacterial activity of biosynthesized Ag-Au nanocomposite

Nanocomposite	**Inhibition zone diameter (mm)**						
	Ag-Au nanocomposite conc. (ppm)			Ag-Au nanocomposite conc. (ppm)			Ciprofloxacin
Tested	*A. fumigatus* ND2 OR636497			*A. flavus* ND1 OR636491			
bacterium	100	200	300	100	200	300	(5 µg)
S. pneumoniae*[*1]	12 ±1	12.5 ±1.5	12 ±1	14 ±1	14.75 ±0.25	15.75 ±1.75	34.5 ±0.5
M. luteus*[*1]	12.5 ±0.5	14.5 ±0	14.5 ±0.5	14.25 ±0.75	14.75 ±0.75	18.75 ±1.25	18 ±1
S. aureus*[*2]	12.5 ±2.5	20.5 ±0.5	20 ±0	10 ±0	10.5 ±0.5	11 ±0.75	35.5 ±0.5
S. aureus*[*3]	11.5 ±0.5	11.5 ±0.5	11.5 ±0.5	11 ±0	11 ±0	11 ±0	32.25 ±1.25
E. coli *[*4]	13.2 ±0.7	12 ±0.5	12.5 ±1.5	12.25 ±0.75	14.25 ±1.25	14.5 ±0.5	32.5 ±0.5
S. typhi*[*5]	10.5 ±0.5	10.5 ±0.5	10.5 ±0	10.75 ±0.25	10.75 ±0.25	13.5 ±1	14.25 ±0.25

***[1]:** clinical isolate, ***[2]:** ATCC 25923, ***[3]:** ATCC 6538, ***[4]:** ATCC 7839 and ***[5]:** ATCC 6539.

Table 3: Antifungal activity of biosynthesized Ag-Au nanocomposite

Nanocomposite Tested	**Inhibition zone diameter (mm)**					
	Ag-Au nanocomposite conc. (ppm)			Ag-Au nanocomposite conc. (ppm)		
Tested fungus	*A. fumigatus* ND2 OR636497			*A. flavus* ND1 OR636491		
	100	200	300	100	200	300
Fusarium oxysporum	9.5 ±0.5	10 ±1	9 ±0	9 ±0.5	10.5 ±0.5	10 ±0
Fusarium solani	9.25 ±0.75	9.5 ±0.5	14.5 ±0.5	8.75 ±0.75	9.5 ±0.5	15.75 ±0.75
Fusarium semitectum	8.5 ±0.5	8.75±0.25	9.25 ±0.75	9 ±1	9.25 ±0.75	9.75 ±0.25
Alternaria solani	15.5 ±0.5	15.5 ±0.5	16.5 ±1.5	9.5 ±0.5	12 ±0	11 ±0
Rhizoctonia solani	8.75 ±0.25	9.5 ±0	12.5 ±2.5	8.25 ±0.25	12.75 ±0.25	15 ±0

Evaluation of cytotoxicity of synthesized Ag-Au nanocomposite: Results of cytotoxicity revealed the lower toxicity of the biosynthesized Ag-Au nanocomposites on the mice bone marrow cells where they lead to (60-75% cell viability) 40 - 25% cell death according to the tested concentration. On the other hand, both samples exert obvious toxic effect against MCF7 cell line with significant IC_{50} values. Ag-Au nanocomposite synthesized by *A. flavus* ND1 OR63649 showed higher toxicity to the MCF7 cells than that exerted by Ag-Au nanocomposite synthesized by *A. fumigatus* ND2 OR63649 where they have reported IC_{50} values of 25.94 and 35.31 µg/mL, respectively as illustrated in the dose response curves, Figure 9.

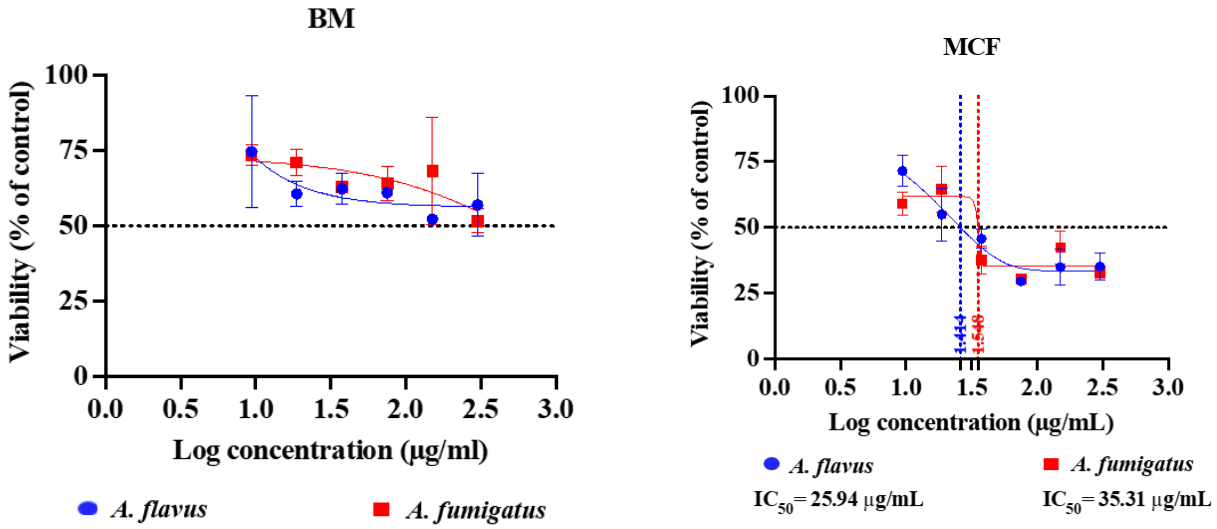

Figure 9: Dose response curves of Ag-Au nanocomposite samples on mice bone marrow cells and MCF7 cell line using MTT assay.

DISCUSSION:

Green synthesis of Ag-Au bimetallic nanocomposite and the evaluation of their biological activities has been investigated in this study. The biosynthesis process has been carried out by new *Aspergillus* fungal isolates. Two Fungal isolates have been isolated from soil samples collected from the Iron and Steel Factory in Helwan-Egypt (29°46'47" N, 31°19'27" E). These isolates have been identified by sequencing their ITS regions. Analysis of the amplified sequences revealed that the first isolate shows high similarity percent with different *Aspergillus fumigatus* strains that present with it in a common cluster according to the phylogenetic tree analysis. On the other hand, the second isolate shows high similarity percent with different *Aspergillus flavus* strains, and it is clustered with them in a common clade. This identification was confirmed by checking their morphological and microscopical features that were found to fit these molecular identification data. Hence these isolates were identified as *Aspergillus fumigatus* isolate ND2 and *Aspergillus flavus* isolate ND1 and their sequences were submitted under the accession numbers of OR636497 and OR636491 respectively in the GenBank.

Water extracts of the obtained biomass of these isolates were tested for their abilities to mediate Ag-Au nanocomposite biosynthesis. Synthesis of Ag-Au nanocomposite was validated by employing different methods. The first level of confirmation for a successive nanoparticles production is the visual observation of a color change and monitoring its UV-Vis absorption spectra to detect the appearance of the characteristic plasmon absorption beak. Upon the addition of the

biomass water extract, a visible color change "to a reddish-brown" has been observed which reflects the reduction of the Ag^{+1} and Au^{+4} ions to the corresponding zero-state nanocrystals. Results of previous studies have clearly shown that the high Ag concentration in the produced nanocomposite can lead to a browner sample color [28]. Estimation of the UV-Vis spectrum revealed the formation of new absorption beak in between the typical positions of absorption beaks that are characteristic for single Ag and Au nanoparticles that are formed at ~ 410 and 540 nm respectively [29-31]. It has been documented that Ag-Au nanocomposite plasmon absorption beak is formed in between the typical positions of absorption peaks of Ag NPs and Au NPs. The exact position of this beak depends on the molar ratio of Au to Ag in the produced nanocomposite [30]. Studies have proven that Ag-Au absorption beak shows an obvious blue shift in case of an increased percentage of Ag in the produced Au-Ag nanocomposite [28]. The plasmon absorption beak detected for Ag-Au nanocomposites synthesized by *Aspergillus flavus* ND1 OR636491 was obviously formed at 440 nm which can reflect the possible high ratio of Ag in the synthesized nanocomposite as the beak is more shifted towards the typical position of single Ag NPs. Indeed in a previous study, Malathi *et al.*, 2014 have detected the plasmon absorption beak of Au-Ag nanocomposite that was prepared with $Au_{0.25}$: $Ag_{0.75}$ molar ratio at 443 nm that is near the typical position of Ag nanoparticles absorption beak [32]. The position of the absorption beak of Ag-Au nanocomposite is also affected by other factors such as the particle size and the dielectric constant of the medium [31].

Size, topographical features, and elemental content of the produced nanoparticles have been monitored utilizing TEM, SEM, and EDX analysis. TEM micrographs revealed the formation of sphere-like polyhedron nanoparticles in both samples and their size ranges between 10-25 nm. Previously, spherical-shaped Au–Ag nanocomposite has been synthesized using *Fusarium semitectum* and 95% of these particles have recorded their size in 10-35 nm range [31]. Also, Au-Ag nanocomposite synthesized by *Mariannaea* sp. HJ showed spherical and pseudo-spherical shapes with 16-19 nm size range [28]. On the other hand, Christina *et al.*, 2024 synthesized sphere-like Ag-Au bi-metallic nanocomposite with size range 9-27 nm using waste orange peel extract [33]. Also, Velpula *et al.*, 2021 have synthesized Ag-Au nanocomposite with similar size range "23 ± 10.3 nm" utilizing gum kondagogu [34], while Ashtari *et al.*, 2023 have tested the ability of galangin of *Suaeda maritima* to mediate the biosynthesis of Ag-Au nanocomposite but the produced nanocomposite has recorded larger size range (45 nm) [19]. SEM imaging revealed that the truncated tetrahedron pattern is the most common topographical pattern found among the biosynthesized nanoparticles in both samples. Energy Dispersive X-ray Spectroscopy (EDX) analysis has been utilized to estimate the elemental content of the biosynthesized nanocomposites and check the percentage of silver and gold in them. EDX spectra of both samples showed the appearance of the absorbance beaks correlated to the surface plasmon resonance of silver and gold nanocrystals and that confirms the successful synthesis of Ag-Au nanocomposite and the incorporation of both metals in the produced nanoparticles. However, the estimated silver and gold content are greatly varied in the prepared samples. Gold was the major metal in the nanocomposite synthesized by *Aspergillus fumigatus* ND2 OR636497 (Ag:Au = 8.21:60.56 %) while silver is the major metal in the nanocomposite synthesized *Aspergillus flavus* ND1 OR636491 (Ag:Au = 55.92: 5.56 %). Other beaks for C, Na, Ca and Mg have been reported in the obtained EDX spectra that may be due to the nature of biomolecules that involved in capping of nanoparticles. Recently,

orange peel extract has been utilized for the formation of Ag-Au nanocomposite that contains 52.1: 35.1 percent ratio of silver and gold respectively [33]. Also, the extract of *Hippeastrum hybridum* has been utilized in the synthesis of Ag-Au bimetallic NPs and the obtained nanocomposite has recorded 12:38.26 % ratio of silver and gold respectively [6].

The functional groups and chemical nature of compounds associated with the biosynthesis and stabilization of the biosynthesized Ag-Au nanocomposite were interpreted by employing FT-IR spectroscopy. FT-IR spectra of both samples showed the common band at 3420 cm^{-1} that is related to bonded O-H stretch [35- 37]. Also, important common bands were observed at ~2920, 2860 and ~1391 cm^{-1} that correspond to C-H and C-H_2 stretching [35-39], and a further beak was observed at ~1625 that reveals the presence of aromatic combinations and C═C aromatic ring stretching vibration (Aryl-substituted C═C). Additionally, the common beak that observed at ~1046 cm^{-1} reflects the presence of C-OH stretch [35-37, 40]. These detected signals support the possible involvement of similar compounds in synthesis and capping of the biosynthesized Ag-Au nanocomposite in both samples that likely involve flavonoids [38], aromatic and alcoholic compounds.

However, a unique band has been reported at ~785 cm^{-1} in FT-IR spectrum of nanocomposite synthesized by *Aspergillus fumigatus* ND2 OR636497 that corresponds to C-H bending Di-substituted [41]. Also, a further unique band has been reported at ~1430 cm^{-1} in FT-IR spectrum of nanocomposite synthesized by *Aspergillus flavus* ND1 OR636491 that is correlated with methyl C-H bend [42].

Bands that are observed at ~ 2375 and 3755 cm^{-1} may be correlated to O=C=O stretching of CO_2 that entrapped on the cavities [43] and to nonbonded hydroxyl group O-H [35-36] stretch of residual water that surrounds the nanoparticle, respectively.

Zeta potential analysis has estimated the presence of a negative charge on the surface of biosynthesized nanocomposite particles. Both samples recorded good surface charge value (-29.0 ± 2.3 & -27.3 ± 0.4) that can support a reasonable stability for the prepared nano solution over its storage. These synthesized Ag-Au nanocomposites showed significantly higher surface charge values than those reported for Ag-Au nanocomposite synthesized by the gum kondagogu that recorded only − 5.95 ± 11.39 surface charge [34].

The biological activities of the biosynthesized Ag-Au nanocomposites have been evaluated by estimating their antibacterial, antifungal, and cytotoxic effects. The Ag-Au nanocomposites synthesized by both fungal isolates exerted a good inhibitory effect against all tested bacteria. Although 300 ppm concentration of Ag-Au nanocomposite synthesized by *A. flavus* ND1 OR63649 has recorded the best inhibitory effect against *Streptococcus pneumoniae*, *Micrococcus luteus, Escherichia coli,* and *Salmonella typhi*, the tested *S. aureus* strains showed either similar or higher sensitivity towards Ag-Au nanocomposite synthesized by *A. fumigatus* ND2 OR63649. The higher antimicrobial behavior of Ag-Au nanocomposite synthesized by *Aspergillus flavus* ND1 OR636491 can be explained by its higher Ag percent in comparison to nanocomposite synthesized by *A. fumigatus* ND2 OR63649 as it is well documented that, Ag NPs exert higher antimicrobial potential than Au NPs.

Lately, many food-born bacteria have developed a wide antibiotic resistance potential including *Escherichia coli*, *Staphylococcus aureus*, and *Vibrio cholera* [44]. Thus, there is an urgent need to develop new antimicrobial agents with a significant inhibitory potential to overcome the increasing antimicrobial resistance against the available antibiotics and chemical antimicrobials [45].

Recently, the antibacterial activity of Ag-Au nanocomposite synthesized by *Suaeda maritima* has

been evaluated and it recorded good antibacterial activities against *Escherichia coli*, *Klebsiella pneumonia*, *Staphylococcus aureus,* and *Proteus mirabilis* at 100 and 250 ppm concentration [19]. Also, Ag/Au nanocomposite synthesized *Hippeastrum hybridum* extract showed promising antibacterial activity against *Streptococcus pneumonia*, *Micrococcus luteus*, *Staphylococcus aureus*, *Streptococcus pyogenes*, *Bacillus cereus*, *Escherichia coli*, *Klebsiella pneumonia*, and *Serratia marcescens* [6]. Little data are available about the antifungal activities of Ag NPs and Ag-Au nanocomposite as most of the studies were concerned with their antibacterial activities [46]. Hence there is a critical need to evaluate the antifungal activities of such nanoparticles on the broader spectrum of fungal species. The current study has evaluated the inhibitory effect of the biosynthesized Ag-Au nanocomposite against different fungi. It has been found that both nanocomposites have exerted a detectable inhibitory effect against the tested fungal pathogens. Both nanocomposites exerted similar antifungal activities against the tested *Fusarium* species. However, *Alternaria solani* revealed higher sensitivity towards Ag-Au nanocomposite synthesized by *A. fumigatus* ND2 OR63649 and *Rhizoctonia solani* showed higher sensitivity towards the Ag-Au nanocomposite synthesized by *A. flavus* ND1 OR63649. Diem *et al.*, 2020 have reported that the biosynthesized Ag-Au bimetallic samples containing high silver content exerted good inhibitory effect activity against *Magnaporthe grisea* fungi [8]. Another recent study has reported a potential inhibitory effect for a green synthesized Ag-Au bimetallic nanocomposite against *Aspergillus niger*, *Aspergillus fumigatus,* and *A. flavus* [6].

The inhibitory effect of Ag nanoparticles against bacterial cells has been well documented. One suggested mechanism for such an inhibitory effect is the constant discharge of silver ions by Ag-containing nanoparticles [18]. These ions have a high affinity to interact with the bacterial cell membrane leading to its destruction and resulting in uncontrolled cell permeability and a final cell death. Moreover, they tend to interact with phosphorus-containing sulfur molecules including the membrane proteins and intracellular DNA and protein molecules which interfere with the functioning of the cell and its proliferation [14]. On the other hand, Ag nanoparticles are involved in the creation of reactive oxygen species (ROS) yielding an oxidative stress that mediates a potent inhibition for respiratory enzymes and interferes with adenosine triphosphate synthesis and induce cell apoptosis [18, 14].

Apart from Ag nanoparticles, Au nanoparticles are also among the most valuable metals nanoparticles that have been estimated to exert antimicrobial activities [6]. Although Au is a rare and inert metal to microorganisms, after being altered, Au nanoparticles, their antibacterial capabilities can be enhanced as their nano size amplifies their antibacterial effects [14]. As in the case of the other noble metals, antimicrobial activities of Au nanoparticles can be maintained due to the production of the reactive oxygen species (ROS) that induce cell apoptosis. Additionally, oxidative damage, inhibition of enzymes, and alterations in gene expression are among the documented mechanisms that can be involved in the suppression of microbial growth by the nanoparticles of noble metals [17].

Breast cancer is the most common type of cancer worldwide. Twenty to thirty percent of people with early-stage breast cancer relapse with distant metastases, such as liver, brain, lung, or bone metastases, following first standard treatment. The most significant problem with breast cancer treatment worldwide is the need to develop innovative therapies as there are many challenges with the conventional cancer medications, including toxicity, drug resistance, and cost [44]. In a trial

to evaluate the safe applicability of the biosynthesized Ag-Au nanocomposites and their anticancer potential their cytotoxic effect against a normal cell line, mice bone marrow cells, and against another cancer cell line, MCF7, has been evaluated. Results revealed the lower toxicity of the investigated nanocomposites against the mice bone marrow cells as the treated cells showed good viability percentage specially in case of the lower tested concentrations. However, both nanocomposite samples have shown elevated toxicity against MCF7 cell line with significant IC_{50} values. Ag-Au nanocomposite synthesized by *A. flavus* ND1 OR63649 showed slightly higher cytotoxic effect against MCF7 cells than that synthesized by *A. fumigatus* ND2 OR63649 which again can be explained by its higher Ag content. The obtained results reveal that these biosynthesized Ag-Au nanocomposites represent new promising and safe candidates for biological applications including food packaging and biomedical applications.

A previous study has tested the cytotoxicity of Ag-Au nanoalloy synthesized under microwave-assisted irradiation and it has been found that this nanoalloy exerts no cytotoxicity towards RAW264.7, Hela, and LO2 cells [46]. Recently, Ashtari *et al.*, 2023 have evaluated the toxicity of Ag-AuNPs nanocomposites synthesized by galangin of *Suaeda maritima* against MCF-7 and they have reported a significant reduction in MCF-7 cell viability by>50% upon this treatment [19].

Generally, Au NPs represent a promising anticancer agent that showed good size-based cytotoxic behavior against different cancer cells. Researchers have carried out many investigations to explain Au nanoparticles cytotoxic behavior. It has been found that the Au NPs exert cytotoxic effects via ROS production and induction of DNA breaking, mitochondrial dysfunctioning, and activation of cell apoptosis cascade [47]. On the other hand, many studies have proved the cytotoxic potential of Ag nanoparticles. This behavior was also explained by its modulated oxidative stress, DNA and mitochondria damage in addition to the induction of cell cycle arrest and the activation of cell apoptosis [13].

CONCLUSION:

The current study has estimated the efficiency of new *Aspergillus fumigatus* and *Aspergillus flavus* isolates to synthesis Ag-Au nanocomposite. Although the biosynthesized nanocomposites showed similar size and morphological features, they reported a variable metallic content. Gold was the major metal in the nanocomposite synthesized by *A. fumigatus* ND2 OR636497 while silver is the major metal in the nanocomposite synthesized *A. flavus* ND1 OR636491. Both nanocomposites showed good antibacterial, antifungal, and anticancer activities with slight variability as a result of the variation in their silver and gold content. This is the first study that utilized *A. fumigatus* and *A. flavus* isolates for Ag-Au nanocomposite biosynthesis. This study aimed to estimate the antimicrobial potential of the synthesized Ag-Au nanocomposites and evaluate their cytotoxicity to assess their applicability in the food packaging systems and in the biomedical field.

Abbreviations: IC50: Half-Maximal inhibitory concentration, MCF7: Michigan Cancer Foundation-7, NPs: Nanoparticles, PDA: Potato Dextrose agar medium, PCR: Polymerase Chain Reaction, SPR: Surface plasmon resonance, TEM: Transmission electron microscopy, FT-IR: Fourier-transform infrared, SEM: Scanning electron microscopy, ATCC: American Type Culture Collection, EDX: Energy Dispersive X-Ray Analyzer, MTT: 3-(4,5-Dimethylthiazol-2-yl)-2,5-Diphenyltetrazolium Bromide.

Author contributions: Design of study and conceptualization; Nashwa H. Abdullah, Ehab B. El

Domany, Mohamed E. Osman. Conducting the practical work and methodology; Dalia M. Abdelrahman, Nashwa H. Abdullah. Data analysis and statistics; Dalia M. Abdelrahman, Nashwa H. Abdullah. Resources; Dalia M. Abdelrahman, Nashwa H. Abdullah, Ehab B. El Domany, Mohamed E. Osman, Ahmed H. Mostafa. Writing manuscript draft; Nashwa H. Abdullah. Editing and revision of the final manuscript; Nashwa H. Abdullah, Mohamed E. Osman.

Competing interests: The authors declare that they have no competing interests.

Acknowledgment/Funding: The study has not received any funds.

REFERENCES:

1. Rao RN, Albaseer SS: Nanomaterials in Chromatographic Sample Preparations; Nanomaterials in Chromatography Chapter 7. Elsevier 2018: 201-231. DOI: https://doi.org/10.1016/B978-0-12-812792-6.00007-8.
2. Thakur M, Sharma A, Chandel M, Pathania D: Modern applications and current status of green nanotechnology in environmental industry; In Micro and Nano Technologies Chapter 9. Green Functionalized Nanomaterials for Environmental Applications. Elsevier 2022: 259-281. DOI: https://doi.org/10.1016/B978-0-12-823137-1.00010-5.
3. Arora N, Thangavelu K, Karanikolos GN: Bimetallic Nanoparticles for Antimicrobial Applications. Front. Chem. 2020, 8:412 . DOI: https://doi.org/10.3389/fchem.2020.00412.
4. Kumar S: Structural Evolution of Iron–Copper (Fe–Cu) Bimetallic Janus Nanoparticles during Solidification: An Atomistic Investigation. The Journal of Physical Chemistry 2020, 124, 1: 1053–1063. DOI: https://doi.org/10.1021/acs.jpcc.9b08411.
5. Borah D, Mishra V, Debnath R, Ghosh K, Gogoi D, Rout J, Pandey P, Ghosh NN, Bhattacharjee CR: Facile green synthesis of highly stable, water dispersible carbohydrate conjugated Ag, Au and Ag-Au biocompatible nanoparticles: Catalytic and antimicrobial activity. Materials Today Communications 2023, 37, 107096. DOI: https://doi.org/10.1016/j.mtcomm.2023.107096.
6. Sher N, Alkhalifah DHM, Ahmed M, Mushtaq N, Shah F, Fozia F, Khan RA, Hozzein WN, Aboul-Soud MAM: Comparative Study of Antimicrobial Activity of Silver, Gold, and Silver/Gold Bimetallic Nanoparticles Synthesized by Green Approach. Molecules 2022, 27, 7895. DOI: https://doi.org/10.3390/molecules27227895.
7. Krishnaraj C, Jagan EG, Rajasekar S, Selvakumar P, Kalaichelvan PT, Mohan N: Synthesis of silver nanoparticles using *Acalypha indica* leaf extracts and its antibacterial activity against water borne pathogens. Colloids and Surfaces B: Biointerfaces 2010, 76: 50-56. DOI: https://doi.org/10.1016/j.colsurfb.2009.10.008.
8. Diem PNH, Phuong TNM, Hien NQ, Quang DT, Hoa TT, Cuong ND: Silver, Gold, and Silver-Gold Bimetallic Nanoparticle-Decorated Dextran: Facile Synthesis and Versatile Tunability on the Antimicrobial Activity. Journal of Nanomaterials 2020, Article ID 7195048. DOI: https://doi.org/10.1016/j.colsurfb.2009.10.008.
9. Janik M, Khachatryan K, Khachatryan G, Krystyjan M, Oszcz ¸eda, Z: Comparison of Physicochemical Properties of Silver and Gold Nanocomposites Based on Potato Starch in Distilled and Cold Plasma-Treated Water. Int. J. Mol. Sci. 2023, 24, 2200. DOI: https://doi.org/ 10.3390/ijms24032200.
10. Martirosyan D, Kanya H, Nadalet C: Can functional foods reduce the risk of disease? Advancement of functional food definition and steps to create functional food products. Functional Foods in Health and Disease 2021, 11(5): 213-221. DOI: https://www.doi.org/10.31989/ffhd.v11i5.788.
11. Paidari S, Ibrahim SA: Potential application of gold nanoparticles in food packaging: a mini review. Gold Bulletin 2021, 54:31–36. DOI: https://doi.org/10.1007/s13404-021-00290-9.
12. Bruna T, Maldonado-Bravo F, Jara P, Caro N: Silver Nanoparticles and Their Antibacterial Applications. Int J Mol Sci. 2021, 22(13):7202. DOI: https://doi.org/10.3390/ijms22137202.
13. Wang D, Xue B, Wang L, Zhang Y, Liu L, Zhou Y: Fungus-mediated green synthesis of nano-silver using *Aspergillus sydowii* and its antifungal/ antiproliferative activities. Scientific reports 2021, 11:10356. DOI: https://doi.org/10.1038/s41598-021-89854-5.
14. Rabiee N, Ahmadi S, Akhavan O, Luque R: Silver and Gold Nanoparticles for Antimicrobial Purposes against Multi-Drug Resistance Bacteria. Materials 2022, 15 (1799).

DOI: https://doi.org/10.3390/ma15051799.

15. Nie P, Zhao Y, Xu H: Synthesis, applications, toxicity and toxicity mechanisms of silver nanoparticles. Ecotoxicology and Environmental Safety 2023, 253, 11463. DOI: https://doi.org/10.1016/j.ecoenv.2023.114636
Harada A, Ichimaru H, Kawagoe T, Tsushida M, Niidome Y, Tsutsuki H, Sawa T, Niidome T: Gold-Treated Silver Nanoparticles Have Enhanced Antimicrobial Activity. Bulletin of the Chemical Society of Japan 2019, 92 (2): 297–301. DOI: https://doi.org/10.1246/bcsj.20180232.
16. Rani P, Varma RS, Singh K, Acevedo R, Singh J: Catalytic and antimicrobial potential of green synthesized Au and Au@Ag core-shell nanoparticles. Chemosphere 2023, 317, 137841. DOI: https://doi.org/10.1016/j.chemosphere.2023.137841.
17. Alshameri AW, Owais M: Antibacterial and cytotoxic potency of the plant-mediated synthesis of metallic nanoparticles Ag NPs and ZnO NPs: A review. OpenNano 2022, 8, 100077. DOI: https://doi.org/10.1016/j.chemosphere.2023.137841.
18. Ashtari A, Kazemi N, Ghasemi E, Chamkouri N, Koolivand Z, Dahdouh E, Golzarian F: Gold nanoparticles, silver nanoparticles, and silver-gold nanocomposites using *Suaeda maritima*: Phytochemical analyses, biosynthesis, characterization, and biological activity. Results in Chemistry 2023, 5, 100983. DOI: https://doi.org/10.1016/j.onano.2022.100077.
19. Syed B, Nagendra Prasad MN, Dhananjaya BL, Mohan KK, Yallappa S, Satish S: Synthesis of silver nanoparticles by endosymbiont *Pseudomonas fluorescens* CA 417 and their bactericidal activity. Enzyme and Microbial Technology 2016, 95: 128-136. DOI: https://doi.org/10.1016/j.rechem.2023.100983.
20. Aneja KR: Experiments in Microbiology, Plant Pathology and Biotechnology; 4th ed. new age international pup. Ltd. 2003: 151-152. DOI: https://doi.org/10.1016/j.enzmictec.2016.10.004.
21. Raper KP, Fennell DI: The genus *Aspergillus*; Williams and Wilkins 1965.
22. Kumar PKR, Hemanth G, Niharika PS, Kolli SK: Isolation and identification of soil mycoflora in agricultural fields at Tekkali Mandal in Srikakulam District. International Journal of Advances in Pharmacy, Biology and Chemistry 2015, 4(2): 484-490.
23. Waksman SA: A method for counting the number of fungi in the soil. Journal of Bacteriology 1922, 7(3): 339-341.
24. Mahfouz AM, Essam TM, Amin MA: Enhancement of Microbial Synthesis of Gold Nanoparticles by Gamma Radiation. British Journal of Applied Science & Technology 2016, 17(4): 1-14. DOI: https://doi.org/10.1128/jb.7.3.339-341.1922.
25. Valgas C, Souza SMD, Smânia EF, Smânia Jr A: Screening methods to determine antibacterial activity of natural products. Braz J Microbiol. 2007, 38: 369-380. DOI: https://doi.org/10.9734/BJAST/2016/28030.
26. Riss TL, Moravec RA, Niles AL, Duellman S, Benink HA, Worzella TJ, Minor L: Cell Viability Assays 'Assay Guidance Manual [Internet]'. Eli Lilly & Company and the National Center for Advancing Translational Sciences, Bethesda (MD) 2013. DOI: https://doi.org/10.1590/S1517-83822007000200034.
27. Fang H, Yan Y, Ju Z, Lian S, Pei X, Ma Q, Qu Y: Characterization of Au-Ag nanoparticles biosynthesized by fungus *Mariannaea* sp. HJ. Sheng Wu Gong Cheng Xue Bao. 2019, Nov 25;35(11): 2061-2068. Chinese. PMID: 31814354 DOI: https://doi.org/10.13345/j.cjb.190160
28. AlBab ND, Nam H, Han C, Han M, Chehimi MM, Mohamed, AA: Mechanochemical synthesis of gold-silver nanocomposites via diazonium salts. Inorganic Chemistry Communications 2022, 137, 109231. DOI: https://doi.org/10.13345/j.cjb.190160.
29. Bi N, Zhang Y, Xi Y, Hu M, Song W, Xu J, Jia L: Colorimetric response of lysine-caped gold/silver alloy nanocomposites for mercury (II) ion detection. Colloids and Surfaces B: Biointerfaces 2021, 205, 111846.
30. Sawle BD, Salimath B, Deshpande R, Bedre MD, Prabhakar BK, Venkataraman A: Biosynthesis and stabilization of Au and Au–Ag alloy nanoparticles by fungus, *Fusarium semitectum*. Sci. Technol. Adv. Mater. 2008, 9, 035012. DOI: https://doi.org/10.1016/j.colsurfb.2021.111846.
31. Malathi S, Ezhilarasu T, Abiraman T, Balasubramanian S: One pot green synthesis of Ag, Au and Au-Ag alloy nanoparticles using isonicotinic acid hydrazide and starch. Carbohydrate Polymers 2014, 111: 734-743. DOI: https://doi.org/10.1088/1468-6996/9/3/035012.
32. Christina B, Thanigaimani K, Sudhakaran R, Mohan S, Arumugam N, Almansour AI, Mahalingam SM: Pyto-Architechture of Ag, Au and Ag–Au bi-metallic nanoparticles using waste orange peel extract for enable carcinogenic Congo red dye degradation. Environmental Research 2024, 242, 117625. DOI: https://doi.org/10.1016/j.carbpol.2014.04.105.

33. Velpula S, Beedu SR, Rupula K: Bimetallic nanocomposite (Ag-Au, Ag-Pd, Au-Pd) synthesis using gum kondagogu a natural biopolymer and their catalytic potentials in the degradation of 4-nitrophenol. International Journal of Biological Macromolecules 2021, 190: 159-169. DOI: https://doi.org/10.1016/j.envres.2023.117625.
34. Bettencourt GM-D-F., Degenhardt J, Torres LAZ, Tanobe VOD-A, Soccol CR: Green biosynthesis of single and bimetallic nanoparticles of iron and manganese using bacterial auxin complex to act as plant bio-fertilizer. Biocatal. Agric. Biotechnol. 2020, 30, 101822. DOI: https://doi.org/10.1016/j.ijbiomac.2021.08.211.
35. Arzanlou M, Samadi R, Frisvad JC, Houbraken J, Ghosta Y: Two novel *Aspergillus* species from hypersaline soils of the National Park of Lake Urmia, Iran. Mycol. Progr. 2016. DOI: https://doi.org/10.1007/s11557-016-1230-8.
36. Kebeish RM, El-Sayed AS: Morphological and molecular characterization of L-methioninase producing *Aspergillus* species. Afr. J. Biotech. 2012, 11(87): 15280–15290. DOI: https://doi.org/10.1007/s11557-016-1230-8.
37. Sadhasivam S, Vinayagam V, Balasubramaniyan M: Recent advancement in biogenic synthesis of iron nanoparticles. J. Mol. Struct. 2020, 1217, 128372.
38. Fatemi M, Mollania N, Momeni-Moghaddam M, Sadeghifar F: Extracellular biosynthesis of magnetic iron oxide nanoparticles by *Bacillus cereus* strain HMH1: Characterization and in vitro cytotoxicity analysis on MCF-7 and 3T3 cell lines. J. Biotechnol. 2018, 270: 1–11. DOI: https://doi.org/10.1016/j.molstruc.2020.128372.
39. Sklenář F, Jurjević Ž, Houbraken J, Kolařík M, Arendrup MC, Jørgensen KM, Siqueira JPZ, Gené J, Yaguchi T, Ezekiel CN, Silva Pereira C, Hubka V.: Re-examination of species limits in *Aspergillus* section Flavipedes using advanced species delimitation methods and description of four new species. Stud. Mycol. 2021, 99, 100120. DOI: https://doi.org/10.1016/j.jbiotec.2018.01.021.
40. Nandiyanto ABD, Oktiani R, Ragadhita R: How to Read and Interpret FTIR Spectroscope of Organic Material. Indonesian Journal of Science & Technology 2019, 4 (1): 97-118. DOI: https://doi.org/10.1016/j.simyco.2021.100120
41. Coates J: Interpretation of Infrared Spectra, A Practical Approach; In Encyclopedia of Analytical Chemistry R.A. Meyers (Ed.). John Wiley & Sons Ltd, Chichester 2000: 10815–10837.DOI: https://doi.org/10.17509/ijost.v4i1.15806.
42. Seiferth O, Wolter K, Dillmann B, Klivenyi G, Freund H-J, Scarano D, Zecchina A: IR investigations of CO_2 adsorption on chromia surfaces :Cr_2O_3 (0001)/Cr(110) versus polycrystalline α-Cr_2O_3. Surface Science 1999, 421: 176–190.
43. Abdulqahar FW, Mahdi ZI, Al-kubaisy SHM, Hussein FF, Kurbonova M, El-Said MM, El-Messery TM: Computational study of antiviral, anti-bacterial, and anticancer activity of green-extracted Sidr (Ziziphus spina-Christi) fruit phenolics. Bioactive Compounds in Health and Disease 2023; 6(10):271-291. DOI: https://doi.org/10.1016/S0039-6028(98)00857-7.
44. Pilevar Z, Martirosyan D, Ranaei V, Taghizadeh M, Balasjin NM, Ferdousi R, Hosseini H : Biological activities, chemical and bioactive compounds of *Echinophora platyloba* DC: A systematic review. Bioactive Compounds in Health and Disease 2024; 7(2):95-109. DOI: https://doi.org/10.31989/bchd.v6i10.1192.
45. Jia X, Yao Y, Yu G, Qu L, Li T, Li Z, Xu C: Synthesis of gold-silver nanoalloys under microwave-assisted irradiation by deposition of silver on gold nanoclusters/triple helix glucan and antifungal activity. Carbohydrate Polymers 2020, 238, 116169. DOI: https://doi.org/10.1016/j.carbpol.2020.116169.
46. Saeed Z, Pervaiz M, Ejaz A, Hussain S, Shaheen S, Shehzad B, Younas U: Garlic and ginger extracts mediated green synthesis of silver and gold nanoparticles: A review on recent advancements and prospective applications,' Biocatalysis and Agricultural Biotechnology 2023, 53, 102868. DOI: https://doi.org/10.1016/j.bcab.2023.102868